Inorganic chemistry Research

Article

Synthesis of OMS-2/NaY Zeolite Hybrid Materials as A Catalyst for Oxidation of Phenol

Mojgan Zendehdel,[a,b]* Mahboobeh Haddadi[a] and Zohreh Mortezaei[a]

[a]*Department of Chemistry, Faculty of Science, Arak University, Arak 38156-8-8349, Iran.*
[b]*Institute of Nanosciences & Nanotechnology, Arak University, Arak, Iran.*

Received: May 5, 2021; Accepted: June 27, 2021
Cite This: *Inorg. Chem. Res.* **2021,** *5*, 193-200. DOI:.1022036/icr.2021.287321.1104

Abstract: In this work, K-OMS compound was synthesized and then K was exchanged with Cu. In the second step Cu-OMS introduced to NaY zeolite and the synthesis zeolite/Cu-OMS hybrid materials were characterized by several techniques: Fourier Transform Infrared spectroscopy (FTIR), X-ray diffraction (XRD), thermogravimetric analysis (TGA) and Burner-Emmet-Taller (BET). The results showed that a new structure from zeolite and OMS was obtained. The catalytic activity of zeolite/Cu-OMS was investigated for oxidation of phenol to catechol and hydroquinone in present of hydrogen peroxide (H_2O_2) as oxidant in different solvents. The activity of phenol oxidation decreases in the series Cu-OMS-2/NaY>OMS-2/NaY at mild conditions. The effect of different factors such as amount of catalyst, temperature, type of oxidant and solvent was investigated. Finally, the kinetic of phenol oxidation with excess H_2O_2 over zeolite/M-OMS catalysts at several temperatures (40, 60 and 80 °C) was studied. These catalysts were very stable and could be reused for more than three times. The results showed a pseudo-first order kinetic with respect to phenol and the catalytic reaction occurred via a radical mechanism. Some advantages of this green catalyst are easy purification, environmental friendly, low catalyst loadings and non-toxic nature.

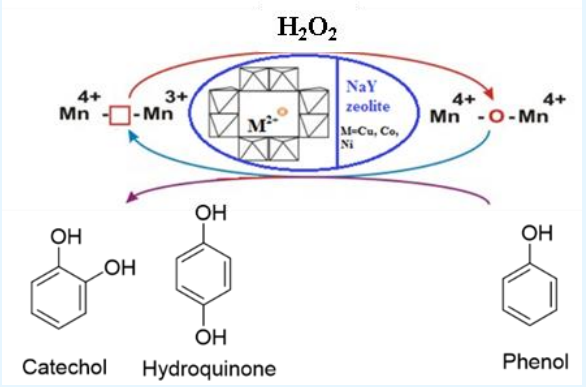

Keywords: Octahedral molecular sieve (OMS-2), Zeolite, Composite, Oxidation of phenol

1. INTRODUCTION

Octahedral molecular sieve (OMS-2), a type manganese oxide, has shown good activity for various oxidation processes and due to the presence of metal ions, OMS-2 structure possesses excellent redox properties. [1-6] K-OMS-2 (mineral name cryptomelane) is constructed from MnO_6 octahedral blocks that form edge-shared double chains and are corner connected to form a tunnel of ~ 4.7 Å by 4.7 Å size. The tunnel has a chemical composition of $KMn_8O_{16}.n H_2O$ with the K^+ cation residing in the center of the tunnel. The material exhibits salient features like mixed-valence (2+, 3+, and 4+) of Mn which creates special properties such as hydrophobic nature, porous structure, easy release of lattice oxygen, and acidic sites.[7-11] Cryptomelane type manganese oxide Octahedral Molecular Sieves (OMS-2) materials are based on edge-shared MnO_6 octahedral hosting both Mn(III) and Mn(IV).[12] The direct doping of OMS-2 by solid-state conversion or aqueous-phase acid synthesis can only be achieved unstable phase, since other more stable manganese phases are usually favored.[13]

Literature review show that the introducing different metal cations such as Ni(II), Co(II), Cu(II), Zn(II), Cr(III), Fe(III), Ti(IV), V(V) and W(VI) has also been accomplished with a variable extent of substitution increase the Lewis acid sites.[14] The OMS show high solubility in polar reaction systems, creating some problems in separation, therfore, many efforts have been made to develop the preparation of stable solid acid catalyst with OMS in water tolerant. The use of this stable water tolerant solid is much easier compared to homogeneous acid catalysts.[15] One approach to improve the catalytic efficiency is heterogeneity of OMS with using of various supports, such as TiO_2/Fe_3O_4. [16]

One of the most important support for creating heterogeneous hybrid catalysts is zeolite which has attracted considerable attention in organic synthesis. [17-19] The zeolite hybrids have many advantages such as suitable acidity, low cost, thermal stability, nontoxic and environmentally safe. Zeolites are crystalline aluminosilicates whose internal voids are formed by cavities and channels of strictly regular dimensions and of different sizes and shapes. In particular, the pore structure of Y zeolite consists of almost spherical 12 Å cavities interconnected tetrahedral through smaller apertures of 7.4

Å diameter. The petrochemical, chemical and pharmaceutical industries produce waste waters containing organics, such as phenols, which are extremely toxic to aquatic life. The phenol and derivatives are generally toxic even at very low concentrations. In general, these pollutions exist in concentration range of 500-10000 ppm, mostly too toxic for conventional biotreatment methods, and too low to treat by combustion. Thus, chemical oxidation emerges as a promising route for phenol removal at intermediate concentrations. The study of the oxidation of phenol catalyzed by peroxides is significantly important for not only it could provide useful information for the elucidation of the reaction mechanism but also be applied in analytical clinical chemistry, in the synthesis of phenolic polymers and in the protection of the environment.[20, 21]
In this aim, for the first time, the OMS-2/NaY and Cu-OMS-2/NaY hybrid materials are synthesied and characterized by XRD, BET, TGA, SEM and FT-IR techniques. The catalytic activity and selectivity of these heterogeneous catalysts as a reusable catalyst was considered to oxidation of phenol.

2. EXPERIMENTAL

All used chemicals were purchased from Merck or Fluka Company. Final product was characterized using X- Ray diffract meter (Philips 8440) with radiation at room temperature *Cu−Ka*, FT-IR (Galaxy series FT-IR 5000 spectrometer), TGA-DSC (Rheometric scientific STA-1500 thermogravimetric analyzer). NMR spectra were recorded on a Bruker (300 MHz) spectrometer. BET was measured with adsorption of nitrogen at 77 K by SIBATA, App, 1100-SA instrument. The yield of product was obtained by gas chromatograph Perkin-Elmer 1800 that equipped with a packed column OV-17 (1.5 m in length) and a flame ionization detector (FID). The Field Emission Scanning Electron Microscope (FE-SEM) photographs of the samples were obtained using a Zeiss Sigma-VP FE-SEM instrument. The chemical compositions of the samples were determined by elemental analysis (Vario E1III).

Preparation of catalysts

Synthesis of NaY and OMS-2

The NaY zeolite was prepared and activated according to the procedure described previously. [22] OMS-2 and Cu-OMS-2 was prepared in our laboratory as follow by the previously reported method. [23-26]

Synthesis of OMS-2/NaY composite

10 mg OMS-2 or Cu-OMS-2 was mixed with 6 mL initial gel of zeolite (with the $16Na_2O$: Al_2O_3: $15SiO_2$: $320H_2O$ molar composition ratio) that aged five days. The mixture was then placed in an autoclave at 100 °C for 24 h. After cooling the reaction mixture to room temperature, the solid was filtered and washed with distillated water until pH 8 and dried in air. The solid products OMS-2/NaY and Cu-OMS-2/NaY hybrid characterized by different methods.

Oxidation of phenol

In a typical reaction, an aqueous solution of 30% H_2O_2 (5.67 g) and phenol (4.7 g) were mixed in 2 mL of MeCN and catalyst (0.025 g). Then, it was heated (80 ºC) and stirred for 8 h. After filtration the solid was washed with solvent. [27,28] The product was subjected to a gas chromatograph Perkin-Elmer 1800 that equipped with a packed column OV-17 (1.5 m in length) and a flame ionization detector (FID).

Calculation of substrates weight percent

Weight percent of each composition can be calculated from the following equation:

$$\%\, S = \frac{(\frac{A_s}{F_s})}{(\sum \frac{A}{F})} \times 100$$

where A_s is the peak area of each composition (cm^2) in GC chromatogram and F_s is the correction factor. For calculation of correction factor, constant amounts (W_s µgr) of phenol, catechol and hydroquinone were subjected to GC analyzer and peak areas were measured. F_s was calculated as:

$$F_s = \frac{(\frac{A_s}{W_s})}{(\frac{A_{benzene}}{W_{benzene}})}$$

Finally, the conversion percent of phenol was calculated from:
% Conversion = 100- % phenol

3. RESULTS AND DISCUSSION

FT-IR analyses were conducted and the results are shown in Figure 1. Figure 1(a-e) shows the spectra of raw OMS-2, Cu-OMS-2, NaY, OMS-2/NaY and Cu OMS-2/NaY, respectively. As shown in Figure 1(a), the two absorption bands near 532 and 713 cm^{-1} is assigned to the asymmetric stretching vibration of the central MnO while the bands at 3400 cm^{-1} are assigned to the stretching vibration of the hydroxyl bond which shift to lower wave number with added Cu.[28] The IR spectra of NaY zeolite (Figure 1b) shows an intense band at ca.1009 cm^{-1} which is attributed to the asymmetric stretching of Al–O–Si chain of the zeolite. The symmetric stretching and bending frequency bands of Al–O–Si framework of the zeolite appear at ca.745 and 440cm^{-1}, respectively.[29] In the FT-IR spectrum of OMS-2/NaY and Cu-OMS-2/NaY hybrid as shown in Figure 1(d and e), the intensity of characteristic bands near 511 and 700 cm^{-1} of OMS-2 and Cu-OMS-2 decreased, which clearly indicates the OMS-2 and Cu-OMS-2 introduce to the pore channels NaY zeolite.
The XRD patterns of OMS-2, Cu-OMS-2 NaY, OMS-2/NaY and Cu-OMS-2/NaY hybrids are presented in Figure 2a-e. Figure 2a shows the XRD pattern with 2θ°= 14 ,18, 28, 37, 42, 50, 60 that confirmed the OMS-2 structure and no significant structural changes were observed with added Cu to it (Figure 2b).[1,30]

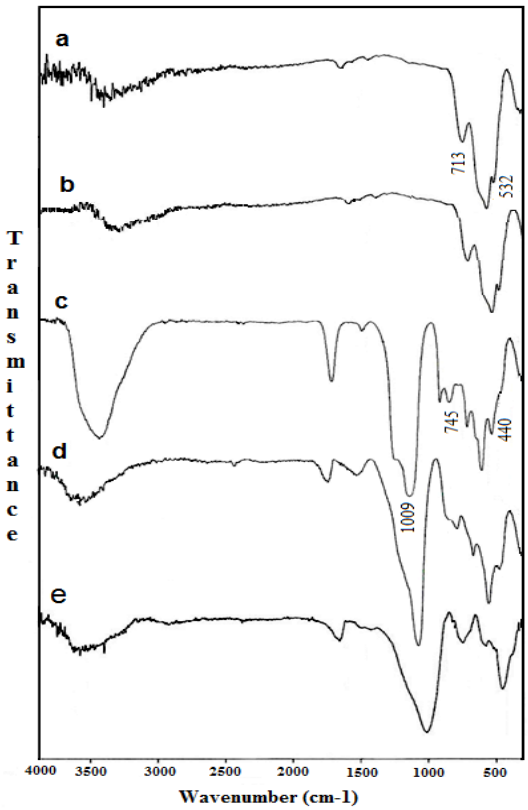

Figure 1. FT-IR spectra for OMS-2 (a) Cu-OMS-2 (b) NaY (c) OMS-2/NaY (d) and Cu-OMS-2/NaY (e).

The characteristic peaks appear at 2θ° of 30.1, 35.5, 43.1, 53.4, 57.0 and 62.6 of Y-zeolite (Figure 2c). Figure 2d-e shows the XRD pattern of OMS-2/NaY and Cu-OMS-2/NaY hybrids. Results demonstrate that both OMS-2 or Cu-OMS and NaY phases present as a hybrid form. As clear, the structure of the zeolite does not collapse upon loading with the OMS. Also, in the higher 2θ region, some diffraction peaks related to NaY and OMS-2 or Cu-OMS-2 with lower intensity can be observed. This decrease can be attributed to the pore-filling effects.[23] Then, it seems there is an amorphous phase in hybrid. The BET data for the sorption capacity of NaY zeolite showed small decrease (from 560 m^2/g to 521 m^2/g and 514 m^2/g) with load of OMS-2 and Cu-OMS, respectively. These results confirmed the trace amount of OMS-2 and Cu-OMS-2 may be incorporated onto pores of zeolite because the pore size is too small. It was also seen that the significant amount of OMS-2 or Cu-OMS-2 is not eliminated upon washing with solvents, which may have attributed to existence of a good interaction between them and NaY in the hybrids.[31]

SEM images of OMS-2, Cu-OMS-2, NaY, OMS-2/NaY and Cu-OMS-2/NaY hybrid catalysts are illustrated in Figure 3a-e. The scanning electron micrograph shows a fibrous needle-like morphology for OMS-2 and after metal addition, agglomerated particle morphology (Figure 3a-b) was seen. [1,32, 33]

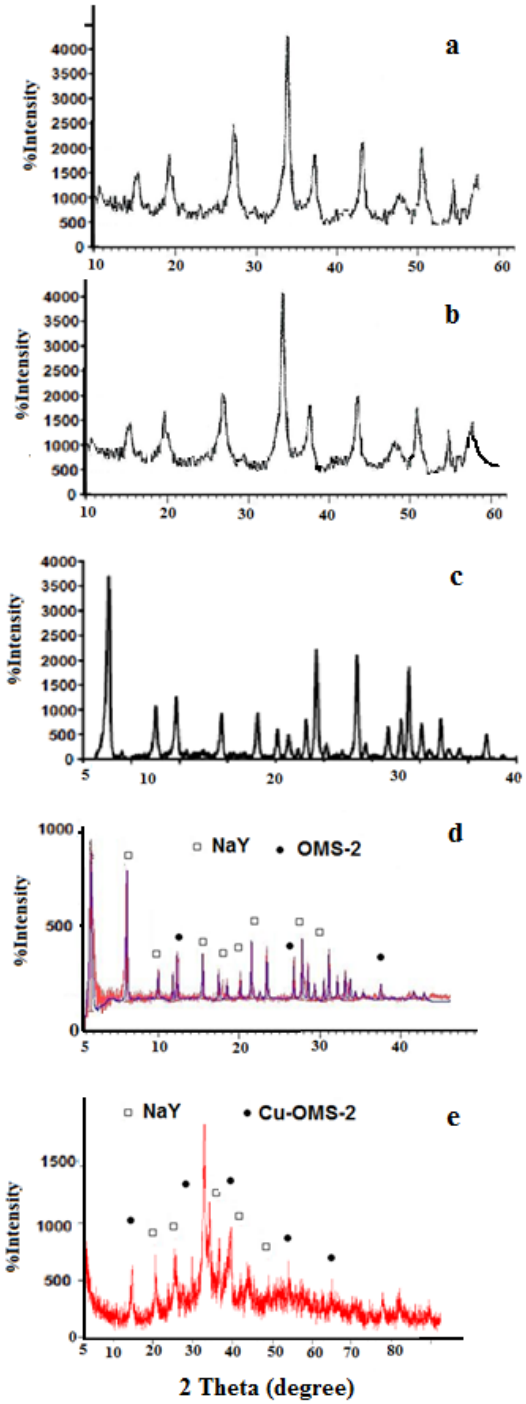

Figure 2. XRD patterns for OMS-2 (a), Cu-OMS-2 (b), NaY (c), OMS-2/NaY (d) and Cu-OMS-2/NaY (e).

Figure 3c show SEM for NaY zeolite that have significant difference in the morphology of some particles after creating OMS-2/NaY and Cu-OMS-2/NaY (Figure 3d-e). It can be seen that the crystal particle size of OMS-2/NaY is approximately 87 nm and for Cu-OMS-2/NaY is about 58 nm. Hence, some of needle-like and agglomerated

particle related to OMS-2 and Cu-OMS-2 is covered with NaY zeolite.[17] The elemental analysis of OMS-2 and Cu-OMS-2 show the presence of Cu w/w % 2.22 and % 2.39, respectively, which confirm introducing copper to OMS and its hybrid with zeolite.

Thermogravimetric analysis profile of parent OMS-2 material synthesized by the reflux method (without metals incorporation) shows initial weight loss in the temperature range between 323 and 350 °C which is due to the removal of water molecules and loss of lattice oxygen present in the sample with a weight loss of 2.2%. The major and second weight loss observed (6.9%) in the temperature between 350 and 680 is due to removal of more lattice oxygen from manganese oxide. This has resulted in manganese oxide OMS-2 phase transformed into lower oxidation state manganese oxide phase such as bixbyite.[34] The third weight loss (1.6%) observed in the temperature range between 680 and 800 °C is due to further decomposition of bixbyite phase into the lower oxidation state such as hausmanite.[35] TGA profiles when metals incorporated to OMS-2 shows the major weight loss shift to higher temperatures above 680 and 800 °C.[35] Figure 4a-b shows TGA/DTA curves of OMS-2/NaY and Cu-OMS-2/NaY hybrids. The TGA/DTA of OMS-2/NaY shows three peaks and the mass losses at 20-300 °C is related to desorption of water (13.52%) of zeolite. The OMS-2 decomposition (7.85%) can be occurred at 300-685 °C. The last step can be related to the further decomposition of OMS-2 and the decomposition zeolite structure about 1.93% at 690-890 °C. The TGA/DTA of Cu-OMS-2/NaY show four peaks, the mass losses at 20-300 °C is related to desorption of water. The peak at 300-695 °C can be assigned to the decomposition of Cu-OMS-2 with mass losses of 7.62%. The third step from 695 to 905 °C with 3.42% weightless is related to the decomposition of HPA. The last step can be related to the decomposition of the structure Cu-OMS-2 and zeolite. It seems that with adding NaY zeolite to OMS-2 or Cu-OMS-2, thermal stability increased.

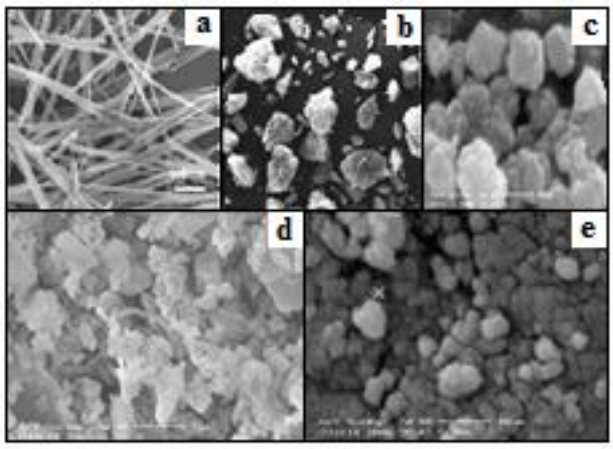

Figure 3. SEM images for OMS-2 (a), Cu-OMS-2 (b) NaY (c) OMS-2/NaY (d) Cu-OMS-2/NaY(e).

Catalytic activity

The hydroxylation of phenol to catechol and hydroquinone with H_2O_2 in CH_3CN in the presence of OMS-2/NaY and M (Cu, Co, Ni) OMS-2/NaY hybrid catalysts was studied and the results are shown in Table 1 and Scheme 1.

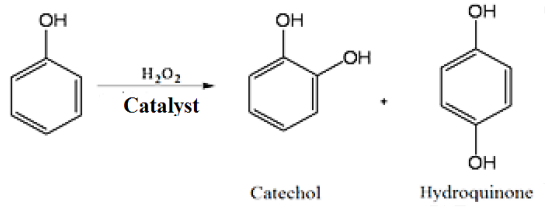

Scheme 1. Oxidation of phenol

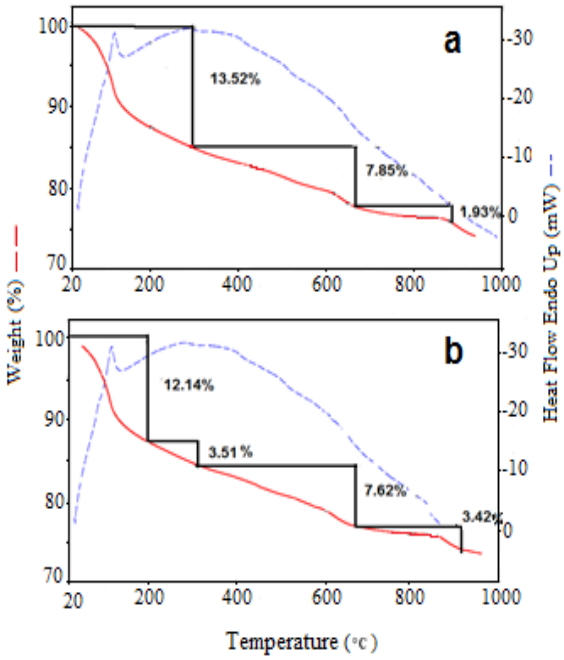

Figure 4. TGA/DTA curves of OMS-2/NaY (a) and Cu-OMS-2/NaY(b) hybrids.

Table 1 shows the oxidation of phenol is negligible in the absence of catalyst and the OMS-2 and NaY have not well catalytic activity. The activity of prepared catalysts for phenol oxidation increases in the series Cu-OMS-2/NaY>OMS-2/NaY. In addition, without using of catalyst, no product for organic reaction can be observed and in the present of NaY and Cu-OMS alon the conversion was lower than 10%.

Table 1. Oxidation of phenol with H_2O_2 catalyzed by different catalysts in CH_3CN and reflux for 6 hours with 0.025 g catalyst.

Catalyst	Conversion(%)	Selectivity(%)	
		Catechol	Hydroquinone
Without Catalyst	8.70	100.00	-
NaY	30.54	65.20	34.80
OMS-2	20.05	59.90	40.10
OMS-2/NaY	58.03	53.62	46.38
Cu-OMS-2/NaY	78.63	60.00	40.00

Table 2. The effect of different solvent in oxidation reaction, reflux for 6 hours with 0.025 g Cu-OMS-2/NaY as catalyst

Solvents	Conversion (%)	Selectivity (%)	
		Catechol	Hydroquinone
Acetonitrile	78.63	60.00	40.00
Chloroform	56.71	53.20	46.80
Dichloromethane	47.83	42.58	57.42
Methanol	31.70	54.63	45.37

In order to achieve suitable reaction conditions for the maximum oxidation of phenol, the catalyst Cu-OMS-2/NaY showed higher activity with CH_3CN solvent compared to other solvents (Table 2). It seems, CH_3CN as a polar solvent was good interactions with phenol, H_2O_2, catechol and hydroquinone, but the solvent with the donor atoms such as methanol have the low activity because set around the metal center. In addition, the present of intramolecular hydrogen bonding in the catechol molecule caused the interaction between catechol and hydroxyl group of zeolite weaker than hydrogen bond in hydroquinone, keeping hydroquinone on the surface of the catalyst with hydrogen bond, and increasing the percent of catechol.[36,37] The influence of the volume of solvent (CH_3CN) on the reaction is illustrated in Table 3. It was evidenced that the volume of acetonitrile plays an important role on the percentage of conversion. 2 mL of solvent was found to be the best volume for reaction with 78.63 % phenol conversion. The effect amount of catalyst (shown in Figure 5) shows that the best amount is 0.025 g with highest percent of conversion.

The effect of temperature was studied with keeping other parameters fixed. The results presented in Figure 6 show that the 80 °C gives the maximum hydroxylation yield of phenol. This observation seems to imply that the reaction rate obeys the Arrhenius law. The effect of phenol: H_2O_2 molar ratios (1:1, 2:1, 3:1 and 4:1) was also studied. The 3:1 molar ratio is the best ratio for hydroxylation reaction and further concentration of oxidant is not effective. This result confirmed that a little oxidant is enough to complete the reaction. Also, the result of considering the suitable oxidant showed that H_2O_2 is better than tert-buthyl hydrogen peroxide (Table 4).

Table 3. The influence of the volume of CH_3CN on the reaction reflux for 6 hours with 0.025 g Cu-OMS-2/NaYas catalyst

Amount of solvent (mL)	Conversion (%)	Selectivity (%)	
		Catechol	Hydroquinone
2	78.63	60.00	40.00
4	60.22	50.01	49.99
7.5	56.50	44.10	55.90
15	44.12	43.47	56.53

In recycling study, the catalyst was separated from the reaction mixture after each experiment by filtration, washed with water and dried carefully before using it in the subsequent run. As Table 5 shows, a rather stable conversion could be achieved after four reactions runs. The result showed that the conditions of this catalyst are mild related to other catalysts with fine yield to oxidation reaction.[21] In Figure 7a-b, the FT-IR and XRD of the best catalyst after final run was compared with first run the catalyst which the result showing no change in catalyst structure. The atomic absorption data to find the present of copper in the product solution confirmed that there is no release of cooper from catalyst.

Table 4. The effect of oxidant in CH_3CN on the reaction reflux for 6 hours with 0.025 g Cu-OMS-2/NaY as catalyst

Oxidant	Conversion (%)	Catechol (%)	Hydroquinone(%)
H_2O_2/phenol	65.0	52.0	48.0
H_2O_2/2phenol	66.5	53.5	46.5
H_2O_2/3phenol	78.6	60.0	40.0
H_2O_2/4phenol	62.0	50.0	50.0
TBHP/3phenol	21.0	-	100.0

Table 5. Catalytic activity after 4 runs with 0.025 g Cu-OMS-2/NaY as catalyst

Catalyst	Run	Conversion (%)
Cu-OMS-2/NaY	1	78.63
Cu-OMS-2/NaY	2	73.53
Cu-OMS-2/NaY	3	70.28
Cu-OMS-2/NaY	4	69.85

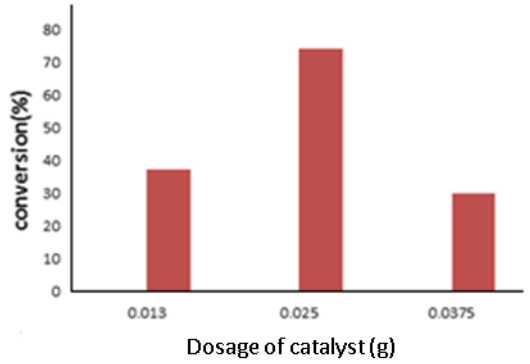

Figure 5. The influence of amount of catalyst on the percentage phenol hydroxylation.

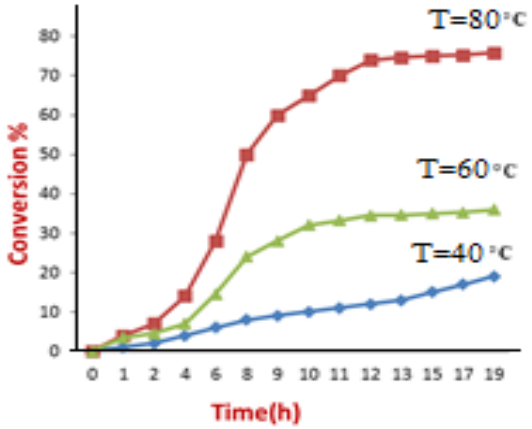

Figure 6. The effect of temperature on phenol conversion (%) for Cu-OMS-2/NaY catalyst.

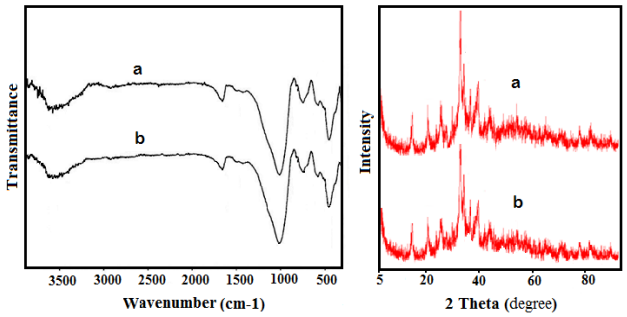

Figure 7. FT-IR spectra (Left) and XRD (Right) of fresh catalyst (a) and the recycled Cu-OMS-2/NaY catalyst (b).

The Scheme 2 illustrates the proposed reaction mechanism. In the first step, based on other works, electron transfer between framework M^{2+} and H_2O_2 will create M^{3+} and $HO^{\bullet}$. This high valence for transition ions is certainly uncommon. In the second step, a radical hydroxyl group introducing into an aromatic ring has been considered as a hallmark of the radical generation. The cycle is closed when M^{3+} is reduced to M^{2+} by the cyclohexadienyl radical derived from phenol converted to catechol and hydroquinone.[38-42]

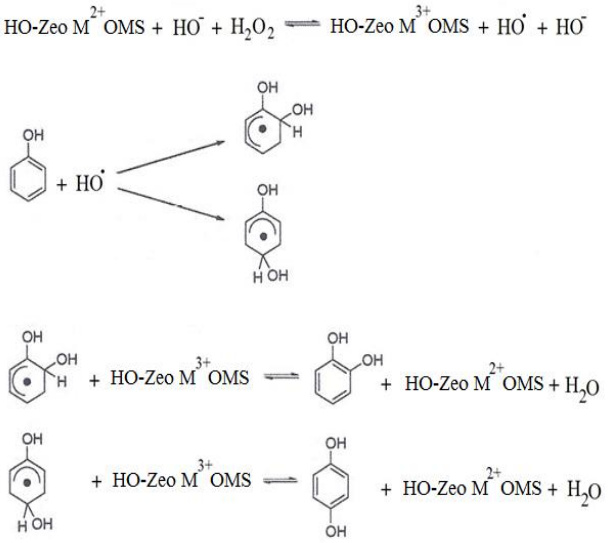

Scheme 2. Mechanism conversion of phenol to catechol and hydroquinone

Kinetic studies

Oxidation of phenol was studied exclusively for kinetic measurements and results of the study are as follows. In this kinetic study, the depletion of phenol concentration in the presence of excess H_2O_2 was monitored and plotted with respect to time (Figure 8).

The reaction was carried out in the presence of 2 mL acetonitrile, 50 mmol phenol, 50 mmol H_2O_2 and 0.025 g of Cu-OMS-2/NaY catalyst at 80 °C in a flask and was analyzed by GC.

The objectives of our kinetics analysis were to determine the reaction rate constant (k), its associated Arrhenius parameters, and the reaction orders for phenol (α), H_2O_2 (β) in Eq. 1:

$$\text{Rate} = k' [\text{phenol}]^{\alpha} [H_2O_2]^{\beta} \quad (1)$$

In order to find α, the rate expression (1) may be rewritten as

$$\text{Rate} = k [\text{phenol}]^{\alpha} \quad (2)$$

If we consider the concentration of H_2O_2 much more than stoichiometric ratio, therefore:

$$[H_2O_2]^{\beta} = \text{constant} \quad (3)$$

and J= -d [phenol]/dt

If α =1 on integrating expression (2), from the initial concentration at initial time to the final concentration at the final time t, the expression (2) can be written as

$$-\text{Ln}(1-X) = k.t \quad (4)$$

That X was the phenol conversion to products and obtained after specific time (t).

$$\text{Ln } k = -E_a/RT + \text{Ln } A \quad (5)$$

To determine the reaction order with respect to phenol, we measured the phenol conversions obtained at different temperatures.[43,44] Then we carried out the integration indicated in Eq. 5 for different integer values for the phenol reaction order and plotted the data as -Ln(1-X) vs. t. According to the expression (4), the plot of -Ln (1-X) with respect to time gives a linear relationship showing a pseudo-first- order dependence on the phenol. The value of α that resulted in a linear plot was selected as the phenol reaction order. Figure 8 displays this integral method plot for a rate law (at 40, 60 and 80 °C) that is first order in phenol (α= 1).

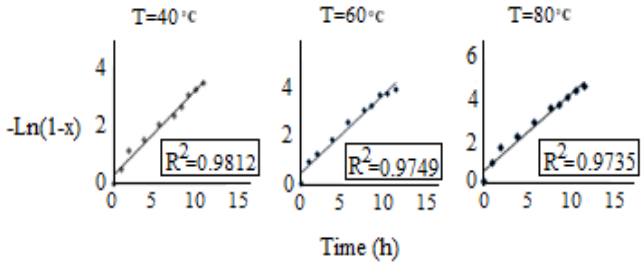

Figure 8. Plots of -Ln(1-x) vs. T for Cu-OMS-2/NaY catalyst at 40 °C, 60 °C and 80 °C

Effect of temperature on the rate of the oxidation of phenol

Oxidation of phenol was carried out at 40, 60 and 80 °C in same reaction condition, and the rate constants of the reactions were found. From the pseudo–first order rate constants, the plot of ln k vs. 1/T (Arrhenius plot) was drawn (Figure 9) and the value of the apparent activation energy (E_a) was evaluated from the slope of the plot, which is 1.415 kcal. mol^{-1}.

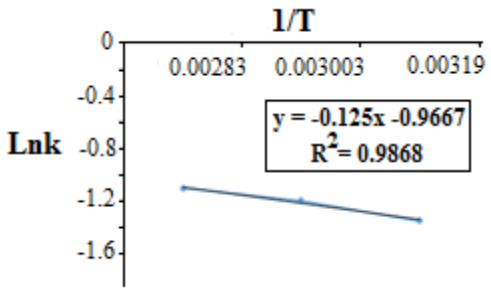

Figure 9. The effect of temperature on the rate constant of the oxidation of phenol (Arrhenius plot).

4. CONCLUSIONS

Through this study, several conclusions have been drawn. In the case of our synthetic method, XRD, FT-IR and SEM indicate that the OMS exists on the external surface of OMS/NaY and Cu-OMS/NaY even after washing with water. In the second section, we consider oxidation of phenol that catalysed by host-guest catalyst with hydrogen peroxide. Results show that percent of product completely depends on catalyst. Also, encapsulated complexes can be recovered and reused without the loss of catalytic activity. The kinetic study of phenol oxidation with excess H_2O_2 over Cu-OMS/NaY catalyst at 40, 60 and 80 °C was investigated which followed a pseudo first order with respect to phenol and the catalytic reaction occurred via a radical mechanism.

CONFLICTS OF INTEREST

There are no conflicts to declare.

AUTHOR INFORMATION

Corresponding Author

Mojgan Zendehdel**:** Email: m-zendehdel@araku.ac.ir, mojganzendehdel@yahoo.com, ***ORCID***: 0000-0003-1364-5660.

Author(s)

Mahboobeh Haddadi, Zohreh Mortezaei

ACKNOWLEDGEMENTS

Thanks to the Research Council of Arak University, Center of Excellence in the Chemistry Department of Arak University for supporting of this work. In addition, special thanks to Prof. Vahid Mahdavi which helped our groups for preparation OMS-2.

REFERENCES

1. R. Kumar, S. Sithambaran, S.L. Suib, *J. Catal*., **2009**, *262*, 304–313.
2. G. D. Yadav, R. K. Mewada, *J. Mol. Catal. A: Chem*., **2013**, *380*, 70–77.
3. G. D. Yadav, R. K. Mewada, *Chem. Eng. Res. Des*., **2012**, *90*, 86-97.
4. N. Yao, X. Bi, L. Zhang, L. Tao, P. Zhao, X. Meng, X. Liu, *Mol. Catal*., **2021**, *504*, 111499.
5. J. Su, C. Cheng, Y. Guo, H. Xu, Q. Ke, *J. Hazard. Mater*., **2019**, *380*, 120890.
6. V. V. Dutov, G. V. Mamontov, V. I. Sobolev, O. V. Vodyankina, *Catal. Today*., **2016**, *278*, 164-173.
7. F. Pan, Y. Yu, A. Xu, D. Xia, Y. Sun, Zh. Cai, W. Liu, J. Fu, *J. Hazard. Mater.*, **2017**, *340*, 36-46.
8. G. D. Yadav, P. A. Chandan, D. P. Tekale, *Ind. Eng. Chem. Res*., **2012**, *51*, 1549–1562.
9. S. Dharmarathna, C. K. King'ondu, L. Pahalagedara, Chung-Hao Kuo, Y. Zhang, S. L. Suib, *Appl. Catal. B: Environ*., **2014**, *147*, 124–131.
10. J. Li, J. Fang, L. Gao, J. Zhang, X. Ruan, A. Xu, X. Li, *Appl. Surf. Sci*., **2017**, *402*, 352-359.
11. X. Li, Q. Zou, Y. Wei, X. Zhou, Z. Wang, A. Xu, X. Ruan, *Appl. Surf. Sci*., **2019**, *497*, 143770.
12. S. L. Suib, *Acc. Chem. Res*., **2008**, *41*, 479–487.
13. J. Cai, J. Liu, W.S. Willis, S.L. Suib, *Chem. Mater*., **2001**, *13*, 2413–2422.
14. M. Ousmane, G. Perrussel, Z. Yan, J.-M. Clacens, F. De Campo, *J. Catal*., **2014**, *309*, 439–452.
15. Y. Izumi, M. Ogawa, K. Urabe, *Appl. Catal. A: General*., **1995**, *132*, 127.
16. T. Zhang, X. Yan, D.D. Sun, *J. Hazard. Mater*., **2012**, *243*, 302–310.
17. M. Zendehdel, A. Mobinikhaledi, H. Alikhani, N. Jafari, *J. Chin. Chem. Soc*., **2010**, *57*, 683-689.
18. M. Zendehdel, A. Barati, H. Alikhani, *Polym. Bull*., **2011**, *67*, 343–360.
19. M. Takeuchi, M. Hidaka, M. Anpo, *J. Hazard. Mater*., **2012**, *237–238*, 133–139.
20. J. Zhang, Y. Tang, J-Qing Xie, J-Zhang Li, W. Zeng, Ch-Wei Hu, *J. Serb. Chem. Soc*., **2005**, *70*, 1137–1146.
21. M. Kurian, R. Babu, *J. Environ. Chem. Eng.*, **2013**, *1*, 86–91.
22. D.W. Breck, N.Y. Tonawanda, Assigned to Union Carbide, Pat. No.3130007, patented April, **1964**, p. 21.
23. M. Abecassis-Wolfovich, R. Jothiramalingam, M.V. Landau, M. Herskowitz, B. Viswanathan, T. K. Varadarajan, *Appl. Catal. B: Environ*., **2005**, *59*, 91-98.
24. V. Mahdavi, Sh . Soleimani, *Research Bulletin*., **2014**, *51*, 153–160.
25. J. Fang, J. Li, L. Gao, X. Jiang, J. Zhang, A. Xu, X. Li, *J. Colloid Interface Sci*., **2017**, *494*, 185-193.
26. D. S. Pisal, G. D.Yadav, *Mol. Catal.*, **2020**, *491*, 110991.
27. M. R. Maurya, M. Kumar, S. J.J. Titinchi, H. S. Abbo, S. Chand, *Catal. Lett*., **2003**, *86*, 97-105.
28. M. R. Maurya, H. Saklani, A. Kumar, S. Chand, *Catal. Lett*., **2004**, *93*, 121-127.
29. R. Kannan, A. Jegan, A. Ramasubbu, K. Karunakaran, *Dig. J. Nanomater. Bios*., **2011**, *6*, 755- 760.
30. R. M. Barrer, Hydrothermal Chemistry of Zeolite, Academic Press, New York, **1982**.
31. Sh. Sohrabnezhad, A. Pourahmad, M.S. Sadjadi, B. Sadeghi, *Physica. E*.**, 2008,** *40***,** 684-688.
32. Y. C. Kim, J. Y. Jeong, J. Y. Hwang, S. D. Kim, S. C. Yi, W. J. Kim, *J. Mem. Sci*., **2008**, *325*, 252-261
33. N. Jiang, X. Li, X. Kong, Y. Zhao, J. Li, K. Shang, N. Lu, Y. Wu, *J. Colloid Interface Sci*., **2021**, *598*, 519-529.

34. R. Jothiramalingam, B. Viswanathan, T. K. Varadarajan, *J. Mol. Catal. A: Chem*., **2006**, *252*, 49–55.
35. M. I. Zaki, A. K. H. Nohman, G. A. M. Hussein, Y. E. Nashed, *Colloids Surf. A*., **1995**, *99*, 247-253.
36. A. K. H. Nohman and H. M. Ismail and G. A. M. Hussein, *J. Anal. Appl. Pyrol*., **1995**, *34*, 265-278.
37. M. Salavati-Niasari, *Inorg. Chem. Commun*., **2004**, *7*, 963-966.
38. M. Salavati-Niasari, A. Sobhani, *J. Mol. Catal. A: Chem*., **2008**, *285*, 58–67.
39. P. A. Massa, M. A. Ayude, R. J. Fenoglio, J. F. Gonzalez, P. M. Haure, *Lattin Am. Appl. Research*., **2004**, *34*, 133-140.
40. R. M. Wang, C.J. Hao, Y. P. Wang, S. B. Li, *J. Mol. Catal. A: Chem*., **1999**, *147*, 173-178.
41. S. Navalon, M. Alvaro, H. Garcia, *Appl. Catal. B: Environ*, **2010**, *99*, 1-26.
42. A. Eftaxias, J. Font, A. Fortuny, J. Giralt, A. Fabregat, F. Stuber, *Appl. Catal. B: Environ*., **2001**, *33*, 175-190.
43. T. D. Thornton, Ph. E. Savage, *AIChE Journal*, **1992**, *38*, 321-327.
44. A. Fortuny, C. Ferrer, C. Benoa, J. Fon, A. Fabregat, *Catal. Today*, **1995**, *24*, 79-83.